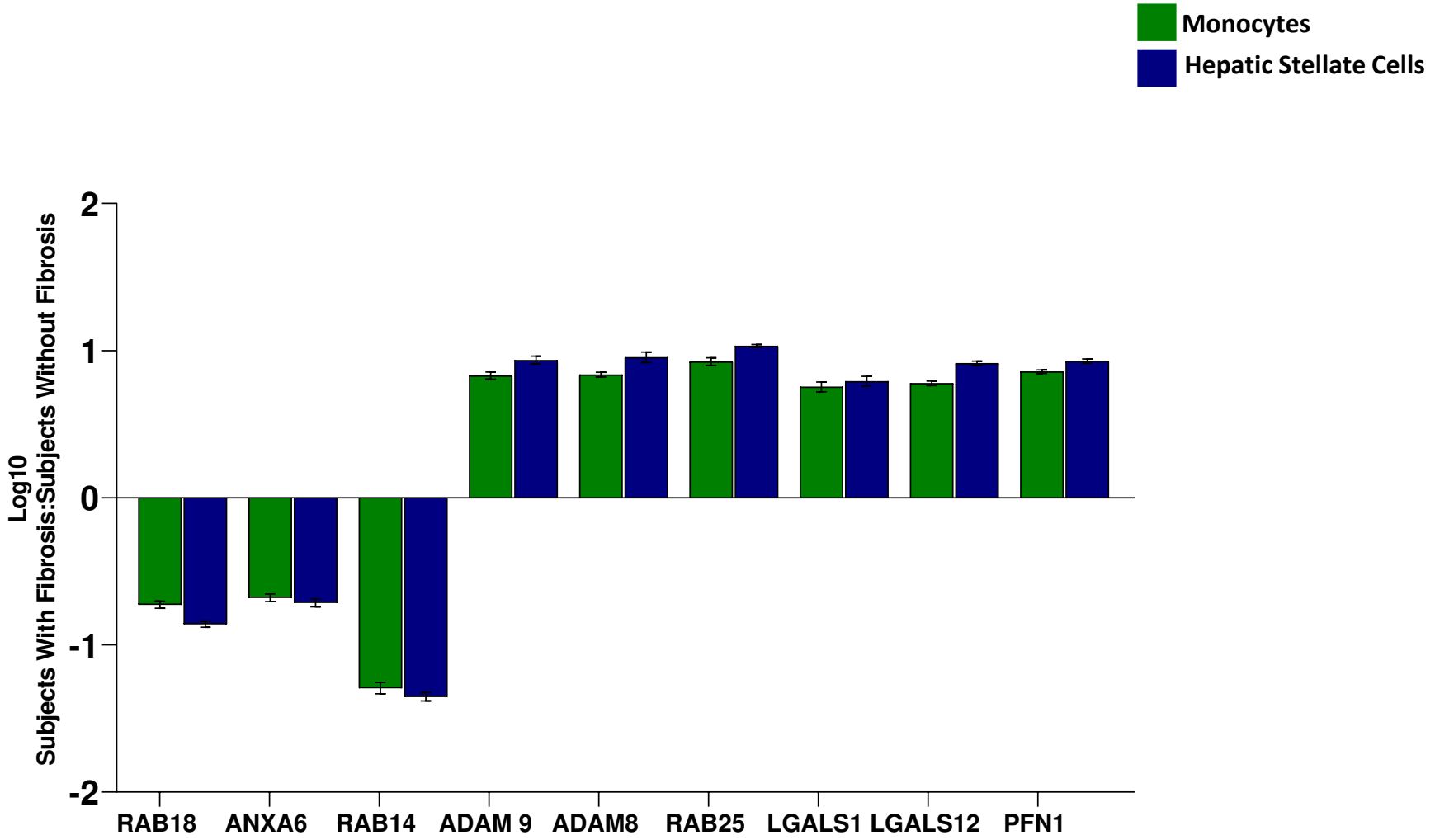
Monocytes
Hepatic Stellate Cells
Log10
Subjects With Fibrosis:Subjects Without Fibrosis
2
1
0
-1
-2
RAB18
ANXA6
RAB14
ADAM 9
ADAM8
RAB25
LGALS1
LGALS12
PFN1

Supplemental Figure 1

iTraQ based analysis of proteins (N=9) differentially expressed in monocytes and hepatic stellate cells (HSCs) of subjects with or without liver fibrosis. Downregulated proteins (N=3) are colored in green while upregulated proteins (N=6) are colored in red.

Ras-related protein Rab-18 (RAB18), Annexin A6 (ANXA6), Ras-related protein Rab-14 (RAB14), Disintegrin and metalloproteinase domain-containing protein 8 and 9 (ADAM 8 and 9), Ras-related protein Rab-25 (RAB25), Galectin 1 and 12 (LGALS1 and 12) and Profilin-1 (PFN1)

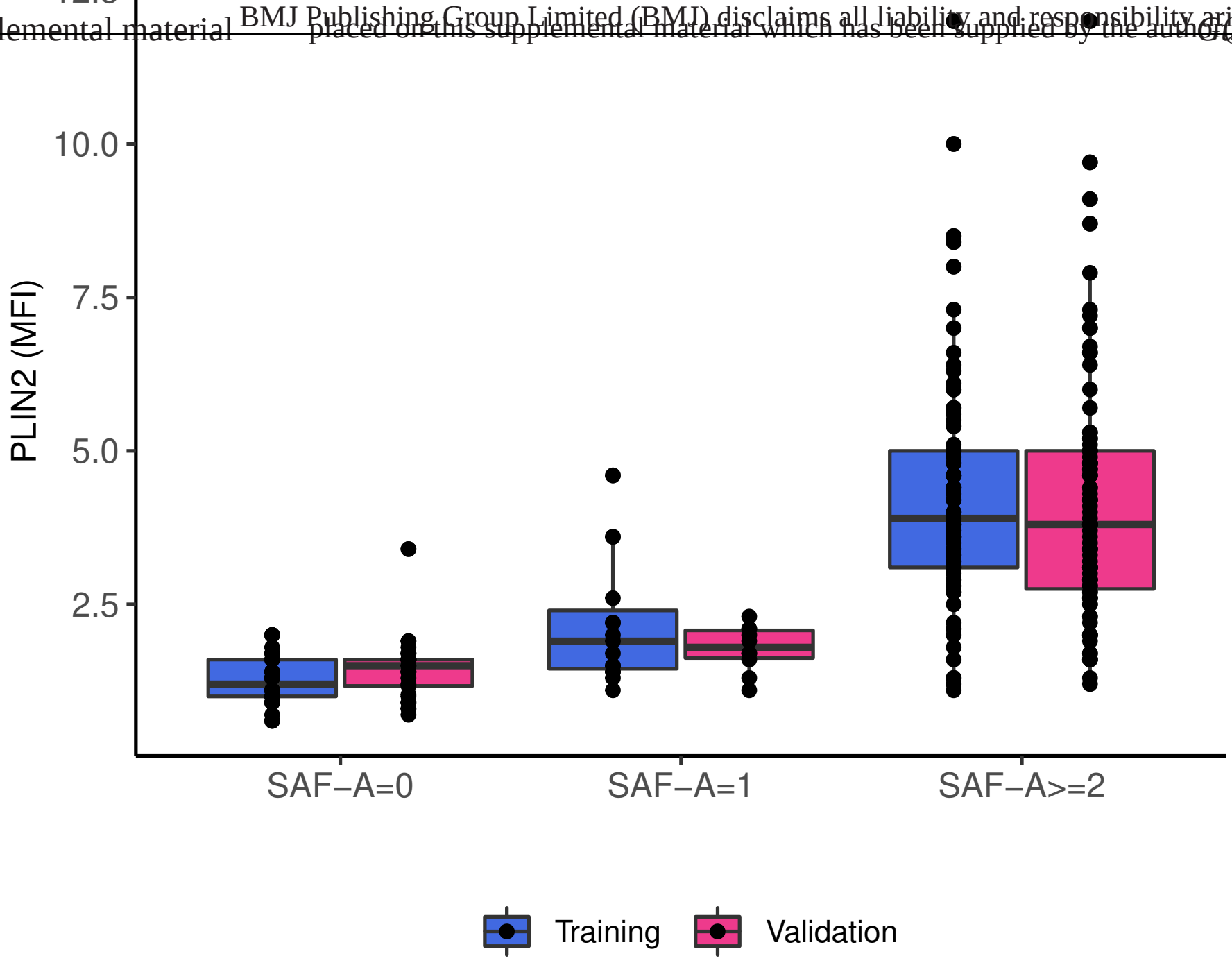
PLIN2 (MFI)
10.0
7.5
5.0
2.5
SAF−A=0
SAF−A=1
SAF−A>=2
Training
Validation

Supplemental Figure 2

Whisker plots of monocyte PLIN2 levels (MFI) measured by flow cytometry in the training and validation cohorts at different levels of SAF-A.

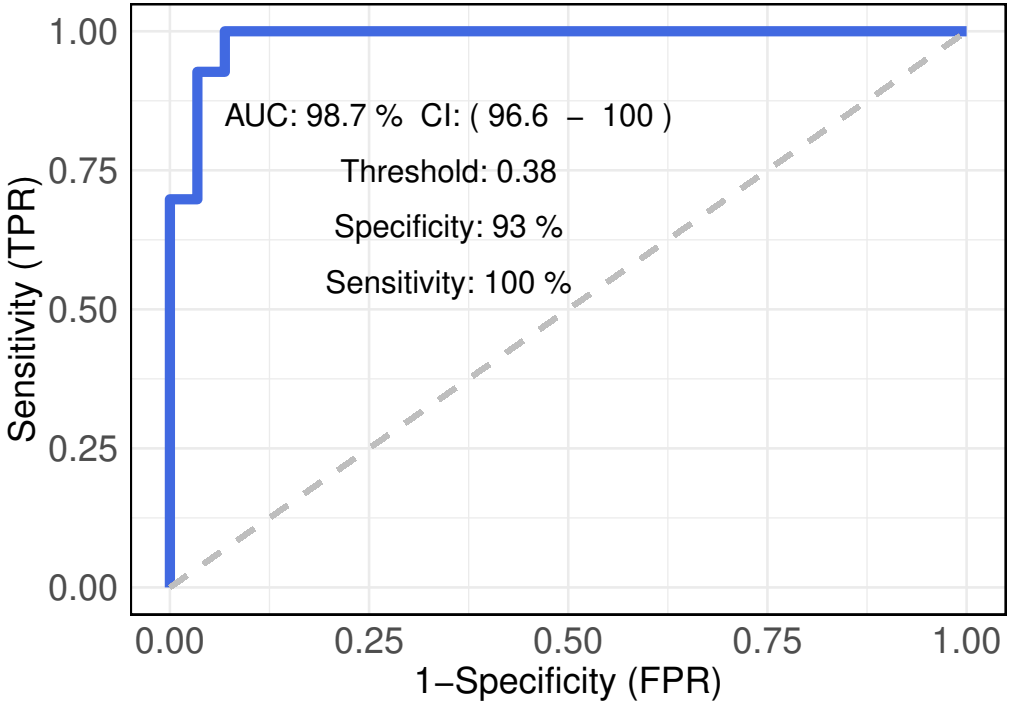
ROC curve
AUC: 98.7 % CI: (96.6 – 100)
Threshold: 0.38
Specificity: 93 %
Sensitivity: 100 %
Sensitivity (TPR)
1−Specificity (FPR)
0.00
0.25
0.50
0.75
1.00

Supplemental Figure 3

ROC curve of PLIN2 algorithm for predicting absence/presence of inflammation (SAF-A=0 vs SAF-A>=1) with the identified threshold, AUROC, sensitivity, and specificity.

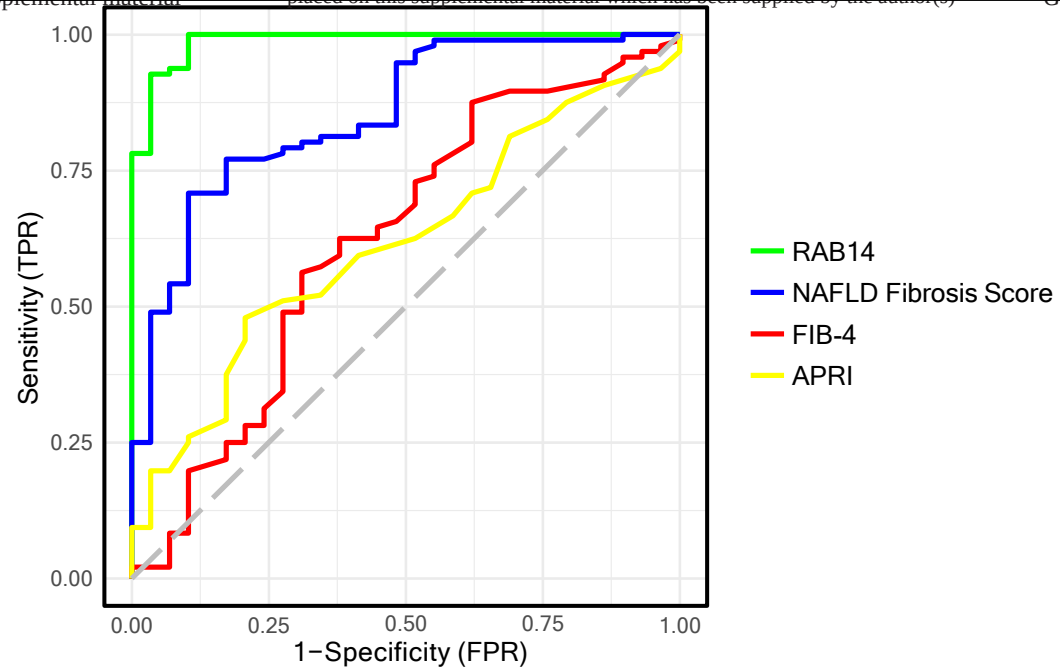
ROC curve
Sensitivity (TPR)
1−Specificity (FPR)
0.00
0.25
0.50
0.75
1.00
RAB14
NAFLD Fibrosis Score
FIB-4
APRI

Supplemental Figure 4

ROC curves for predicting presence/absence of liver fibrosis using the RAB14 algorithm, NAFLD Fibrosis Score, Fibrosis-4 (FIB-4) and AST-to-Platelet Ratio Index (APRI).

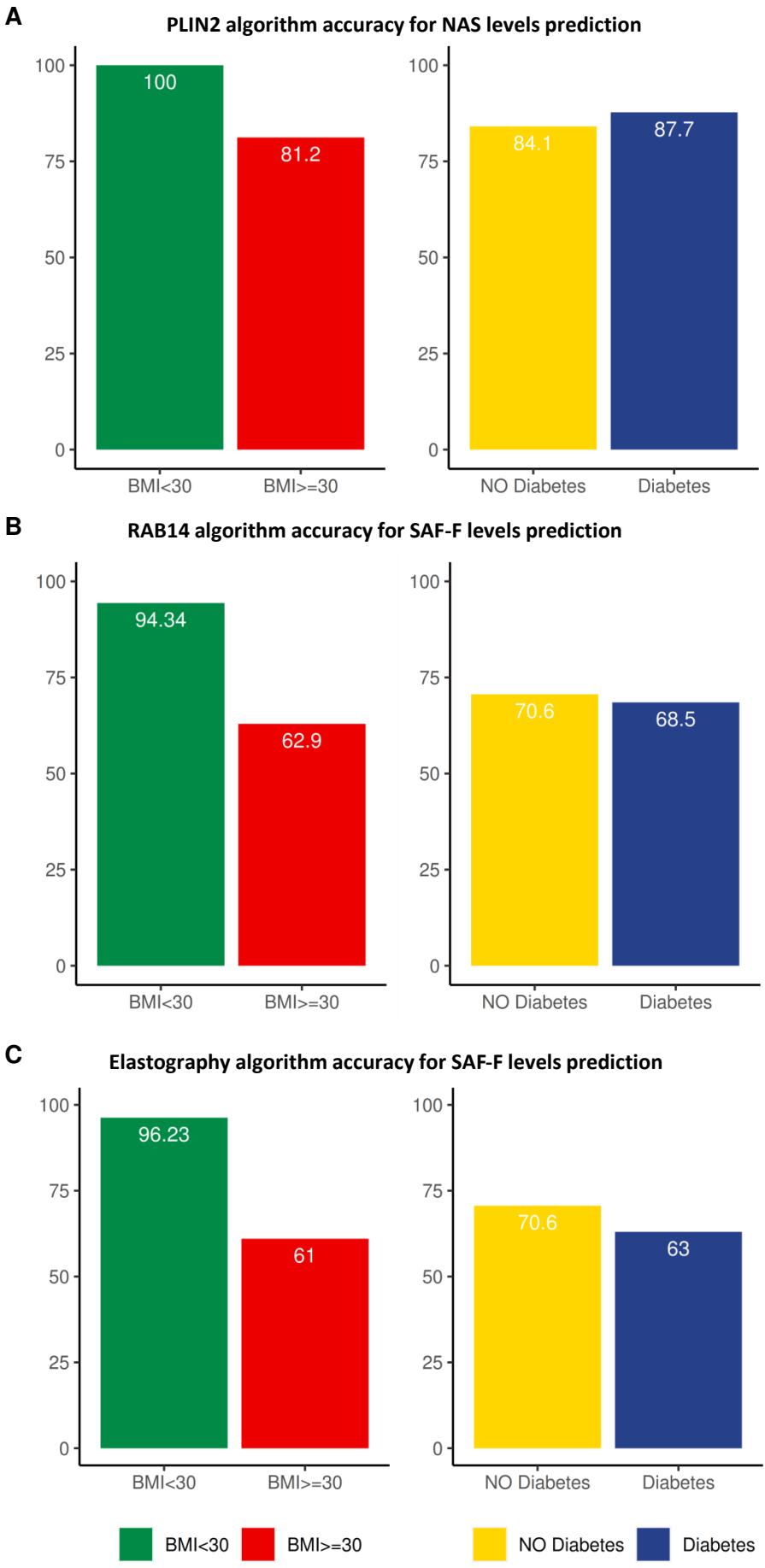
A
PLIN2 algorithm accuracy for NAS levels prediction
100
81.2
84.1
87.7
BMI<30
BMI>=30
NO Diabetes
Diabetes
B
RAB14 algorithm accuracy for SAF-F levels prediction
94.34
62.9
70.6
68.5
C
Elastography algorithm accuracy for SAF-F levels prediction
96.23
61
70.6
63
0
25
50
75
100
BMI<30
BMI>=30
NO Diabetes
Diabetes

Supplemental Figure 5

A: PLIN2 algorithm accuracy for NAS level prediction in subjects with BMI<30 or BMI≥30 (left panel) and in subjects with or without type 2 diabetes (right panel).

B: RAB14 algorithm accuracy for SAF-F level prediction in subjects with BMI<30 or BMI≥30 (left panel) and in subjects with or without type 2 diabetes (right panel).

C: Elastography algorithm accuracy for SAF-F level prediction in subjects with BMI<30 or BMI≥30 (left panel) and in subjects with or without type 2 diabetes (right panel).

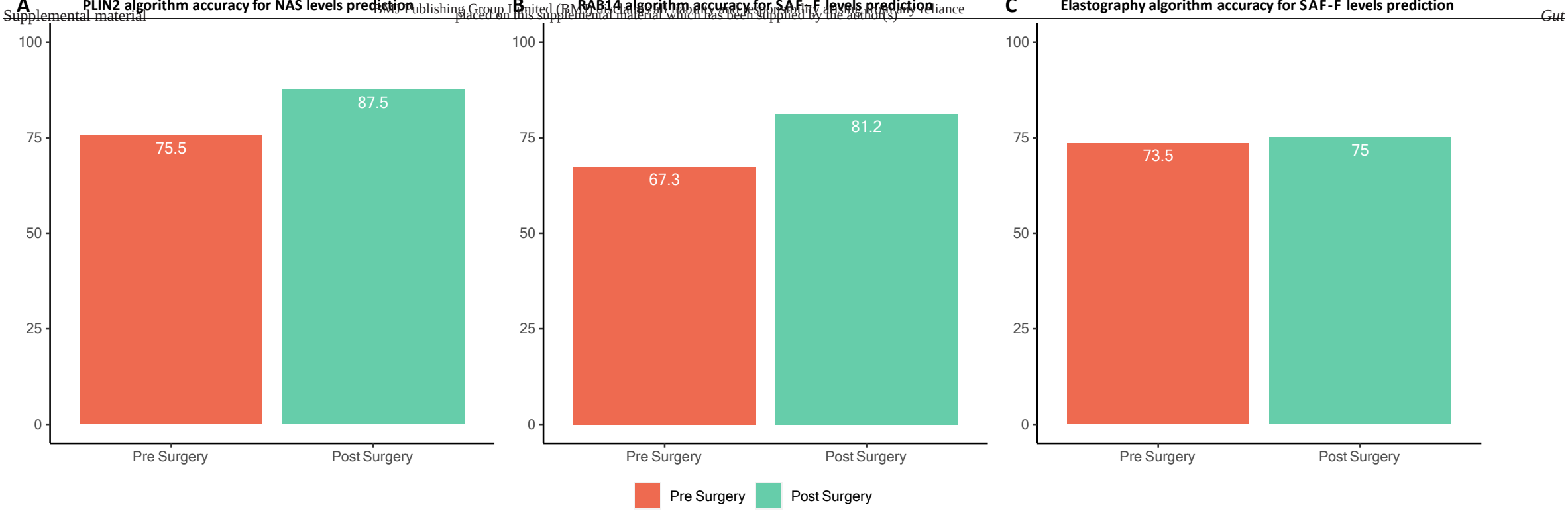
A
PLIN2 algorithm accuracy for NAS levels prediction
B
RAB14 algorithm accuracy for SAF-F levels prediction
C
Elastography algorithm accuracy for SAF-F levels prediction
100
75
50
25
0
75.5
87.5
67.3
81.2
73.5
75
Pre Surgery
Post Surgery
Pre Surgery
Post Surgery

Supplemental Figure 6

A: PLIN2 algorithm accuracy for NAS level prediction in subjects before and after surgery.

B: RAB14 algorithm accuracy for SAF-F level prediction in subjects before and after surgery.

C: Elastography algorithm accuracy for SAF-F level prediction in subjects before and after surgery.

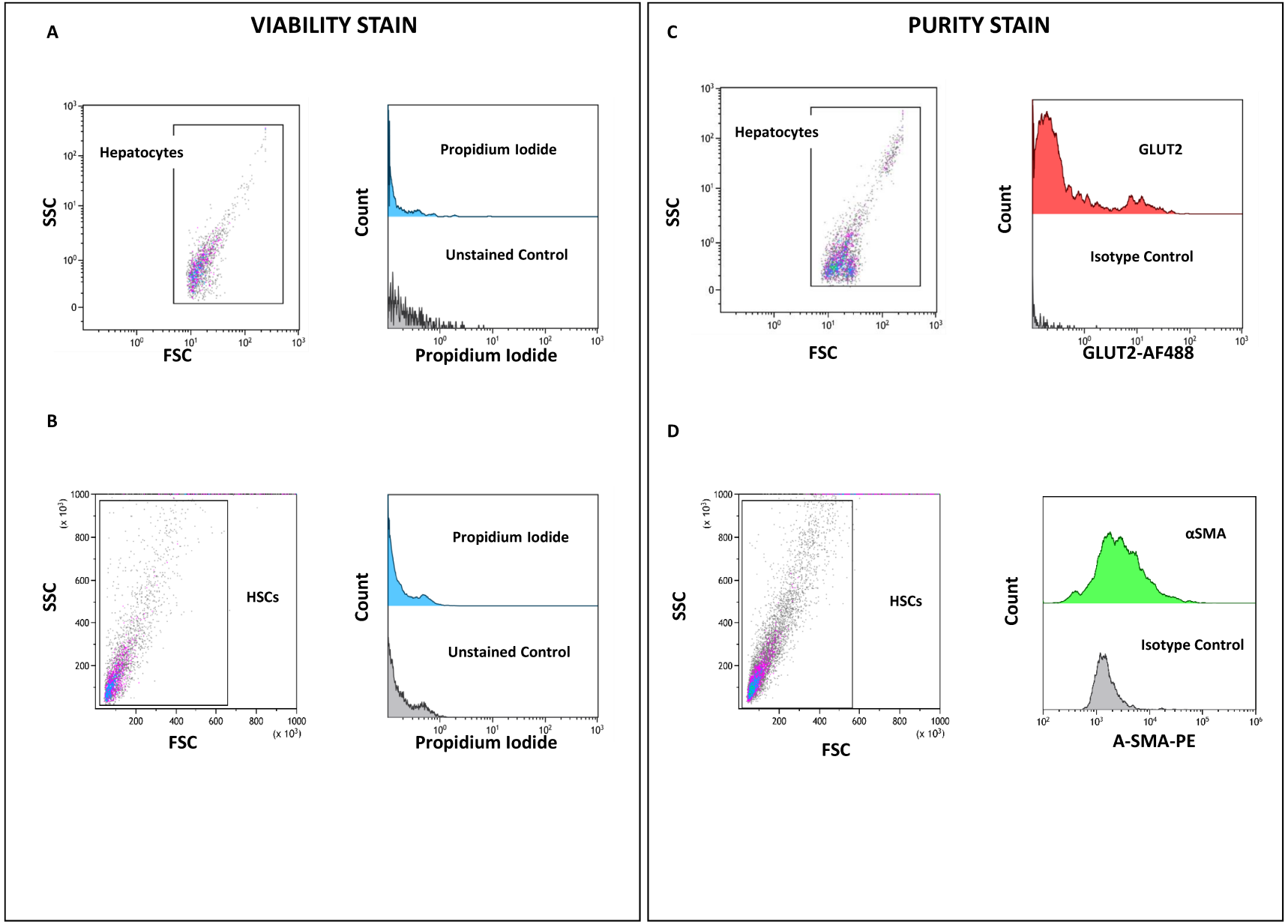
A
VIABILITY STAIN
Hepatocytes
SSC
FSC
Propidium Iodide
Unstained Control
Count
Propidium Iodide
B
HSCs
SSC
FSC
(x 10³)
Propidium Iodide
Unstained Control
Count
Propidium Iodide
C
PURITY STAIN
Hepatocytes
SSC
FSC
GLUT2
Isotype Control
Count
GLUT2-AF488
D
HSCs
SSC
FSC
(x 10³)
αSMA
Isotype Control
Count
A-SMA-PE

Supplemental Figure 7

Cell viability of hepatocytes (A) and hepatic stellate cells (B), stained with propidium iodide and analyzed by flow cytometry.

Cell purity assessed by flow cytometry; primary hepatocytes (C) were stained with GLUT2 Alexa Fluor® 488-conjugated antibody and hepatic stellate cells (D) with α-Smooth Muscle Actin PE-conjugated antibody.

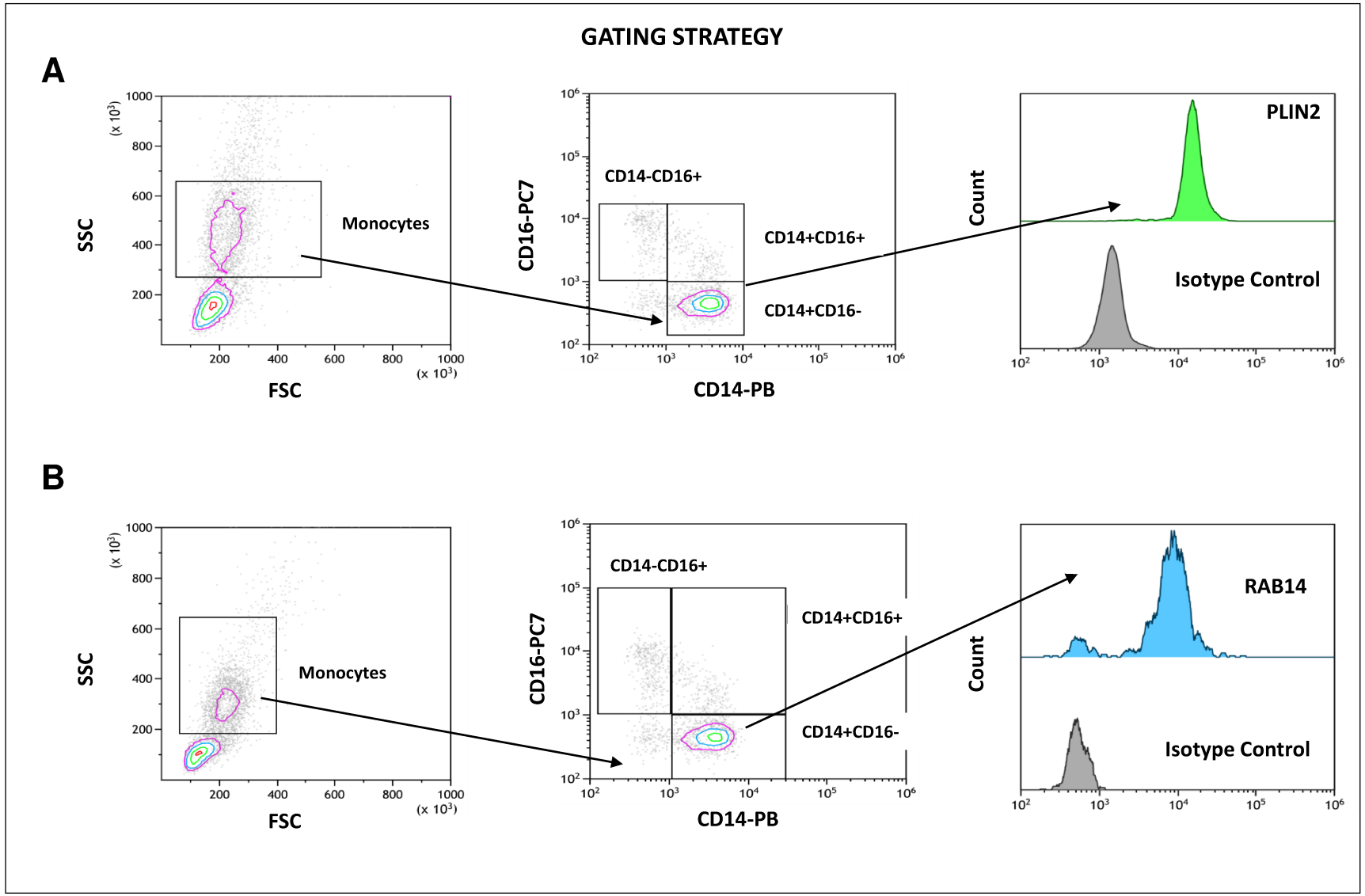
GATING STRATEGY
A
SSC
(x 10³)
FSC
Monocytes
CD16-PC7
CD14-PB
CD14-CD16+
CD14+CD16+
CD14+CD16-
Count
PLIN2
Isotype Control
B
SSC
FSC
Monocytes
CD16-PC7
CD14-PB
CD14-CD16+
CD14+CD16+
CD14+CD16-
Count
RAB14
Isotype Control

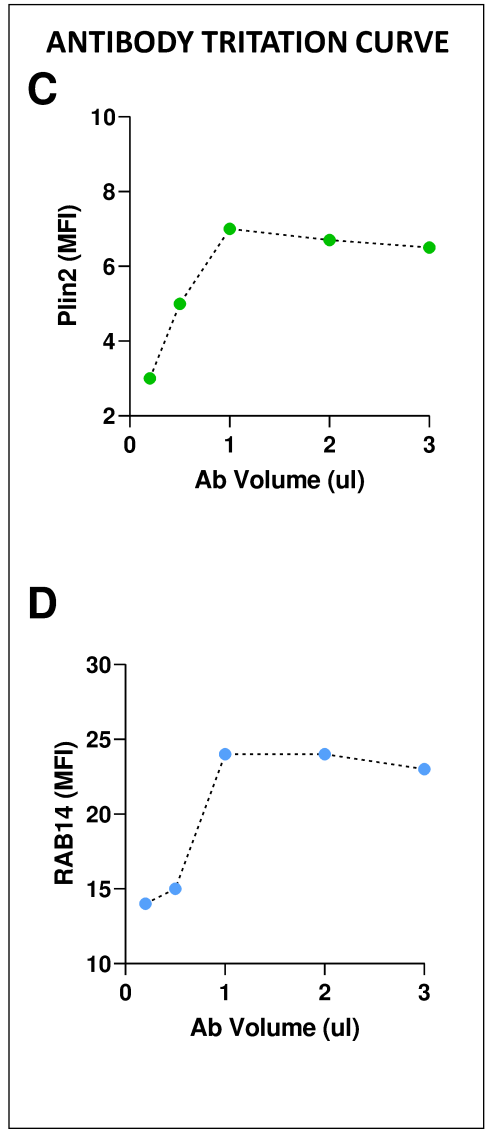
ANTIBODY TRITATION CURVE
C
Plin2 (MFI)
Ab Volume (ul)
D
RAB14 (MFI)
Ab Volume (ul)

Supplemental Figure 8

Gating strategies for PBMCs stained with PLIN2 (A) or RAB14 (B). Antibody tritation curve for PLIN2 (C) or RAB14 (D).

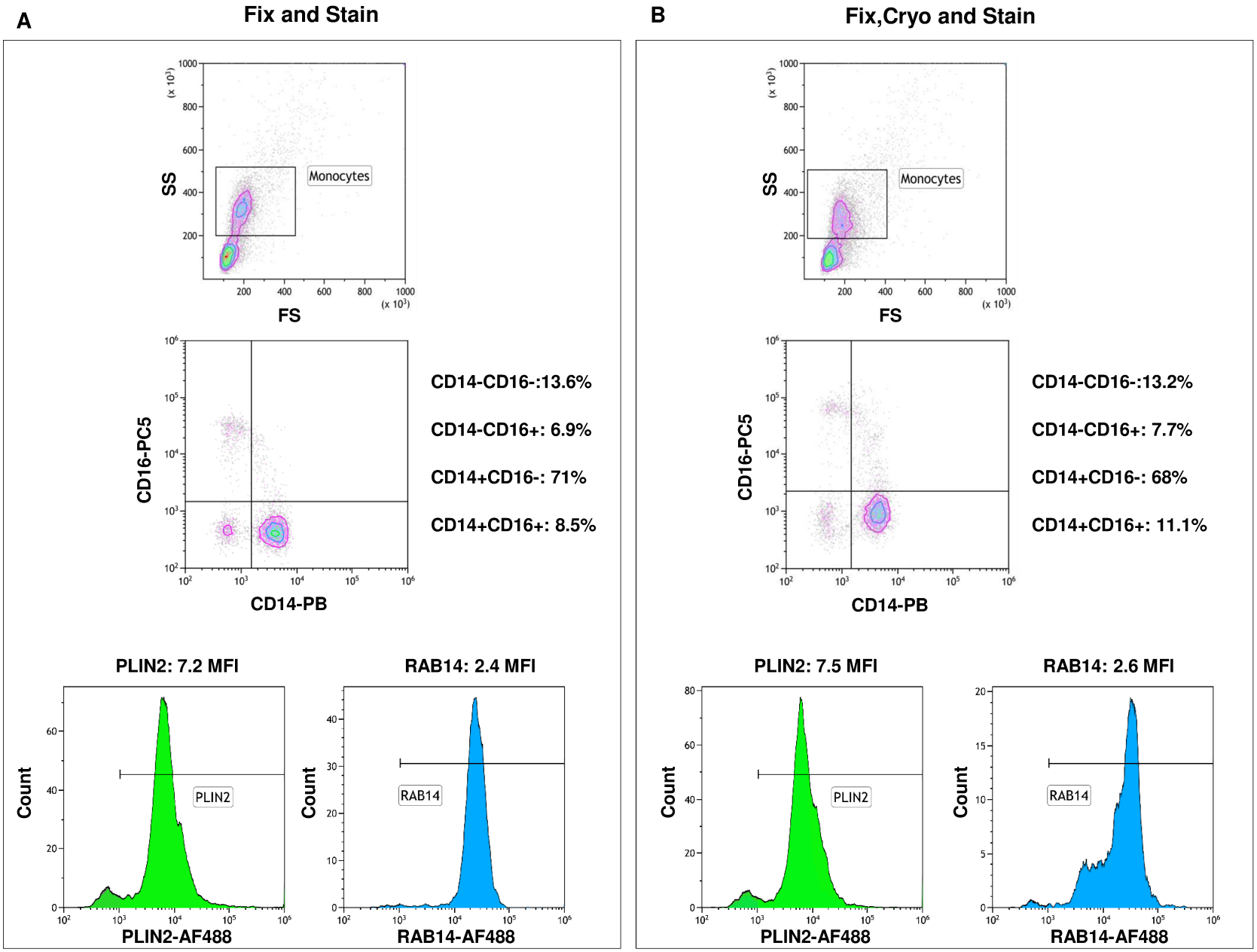
A
Fix and Stain
B
Fix,Cryo and Stain
Monocytes
SS
FS
CD16-PC5
CD14-PB
CD14-CD16-:13.6%
CD14-CD16+: 6.9%
CD14+CD16-: 71%
CD14+CD16+: 8.5%
CD14-CD16-:13.2%
CD14-CD16+: 7.7%
CD14+CD16-: 68%
CD14+CD16+: 11.1%
PLIN2: 7.2 MFI
RAB14: 2.4 MFI
PLIN2: 7.5 MFI
RAB14: 2.6 MFI
Count
PLIN2
RAB14
PLIN2-AF488
RAB14-AF488

Supplemental Figure 9

Influence of the different handling procedures on PBMCs stained for PLIN2 or RAB14. Cells were processed using the following procedures: fixation and staining (A) or fixation, cryopreservation and staining (B).